Chemistry & Biology, Vol. 11, 439–448, April, 2004, ©2004 Elsevier Science Ltd. All rights reserved. DOI 10.1016/j.chembiol.2004.03.021

The First Fluorescent Diboronic Acid Sensor Specific for Hepatocellular Carcinoma Cells Expressing Sialyl Lewis X#

Wenqian Yang,[1] Haiying Fan,[2] Xingming Gao,[1] Shouhai Gao,[1] Vishnu Vardhan Reddy Karnati,[1] Weijuan Ni,[1] W. Borden Hooks,[2] John Carson,[2] Brent Weston,[2,*] and Binghe Wang[1,*]
[1]Department of Chemistry
Georgia State University
33 Gilmer St. S.E.
Atlanta, Georgia 30303
[2]Department of Pediatrics
University of North Carolina
Chapel Hill, North Carolina 27599

Summary

Carbohydrate antigens with subterminal fucosylation have been implicated in the development and progression of several cancers, including hepatocellular carcinoma (HCC). Fluorescent sensors targeting fucosylated carbohydrate antigens could potentially be used for diagnostic and other applications. We have designed and synthesized a series of 26 diboronic acid compounds as potential fluorescent sensors for such carbohydrates. Among these compounds, 7q was able to fluorescently label cells expressing high levels of sLex (HEPG2) within a concentration range of 0.5 to 10 μM. This compound (7q) did not label cells expressing Lewis Y (HEP3B), nor cells without fucosylated antigens (COS7). This represents the first example of a fluorescent compound labeling cells based on cell surface carbohydrate structures.

Introduction

Fluorescent sensors capable of recognizing specific cell-surface biomarkers are useful diagnostics. Our laboratory has been particularly interested in the development of fluorescent sensors for carbohydrates. It is known that cell-surface carbohydrates, as part of glycosylated proteins and lipids, often form characteristic signatures of different cell types [1, 2]. In particular, certain cell surface carbohydrates, such as sialyl Lewis X (sLex), sialyl Lewis a (sLea), Lewis X (Lex), and Lewis Y (Ley) (Figure 1), have been associated with the development and progression of many types of cancers [3–6], including hepatocellular carcinoma (HCC), one of the most common carcinomas worldwide [7].

One specific example associated with the development and progression of human carcinomas is their ability to express α(1,3)-fucosylated carbohydrates, which are important components of ligands involved in selectin-mediated cell adhesion and inflammatory responses [8, 9]. Inflammatory cytokines can increase the metabolic activity and expression of several heavily glycosylated acute phase reactants in HCC [10–14], and some inflammatory molecules appear to be involved in the progression of HCC. Alpha-fetoprotein, for example, is heavily fucosylated in chronic hepatitis and HCC [15]. Normally differentiated hepatocytes do not express sLex, but chronically diseased liver expresses high levels of sLex, and this is associated with a high degree of carcinogenicity [16].

Diagnosis and staging of HCC is often limited due to inability to detect advanced disease. Treatment of HCC is also impaired by lack of sensitive detection and further by drug resistance [17]. Biosensors that could both recognize occult metastasis and provide targeted delivery of treatment could potentially improve chances for success in this disease. Herein, we describe our search for fluorescent diboronic acid compounds that can specifically recognize sLex [18]. One compound was able to fluorescently label HCC lines that express the target carbohydrate. This represents the first example of a small organic molecule being used to fluorescently label cells based on the specific recognition of cell-surface carbohydrate structures.

Results and Discussion

Chemistry

For this project, we selected sLex (Figure 1) as our initial target for sensor design because it is implicated in the development of liver and colon cancer [16, 19]. Critical to the development of high affinity and high specificity sensors for carbohydrates is the need for recognition moieties that have strong interactions with the functional groups, such as hydroxyl groups, on a carbohydrate. It has been known since the 1940s that boronic acids can bind compounds with a diol structural motif with high affinity [20]. By taking advantage of this strong interaction, several molecular recognition systems for carbohydrates based on boronic acid moieties have been developed [21–31]. Recently, our lab has undertaken extensive studies of the interaction of boronic acid and diols and achieved a much greater understanding of the factors that influence this complexation process [32]. Our group has also developed a new method of making fluorescent sensors for sugars through template-directed polymerization of boronic acid monomers [33, 34]. However, most of these early efforts were focused on monosaccharides. Effort in designing sensors for cell-surface polysaccharides has been very limited [35]. Possible reasons for this include the complexity of polysaccharides and their conformational flexibility, which makes sensor construction difficult.

In designing sensors for saccharides, it is essential that binding also trigger a reporting event. It has been known that anthracene fluorescence can be quenched by nitrogen lone pair electrons on an amino group (Figure 2). However, this quenching can be removed or reduced if lone pair electrons are masked through B-N bond formation [23, 36]. Since binding with a carbohy-

*Correspondence: bwwmd@med.unc.edu (Weston); wang@gsu.edu (Wang)
A major part of this work was performed at North Carolina State University, Department of Chemistry.

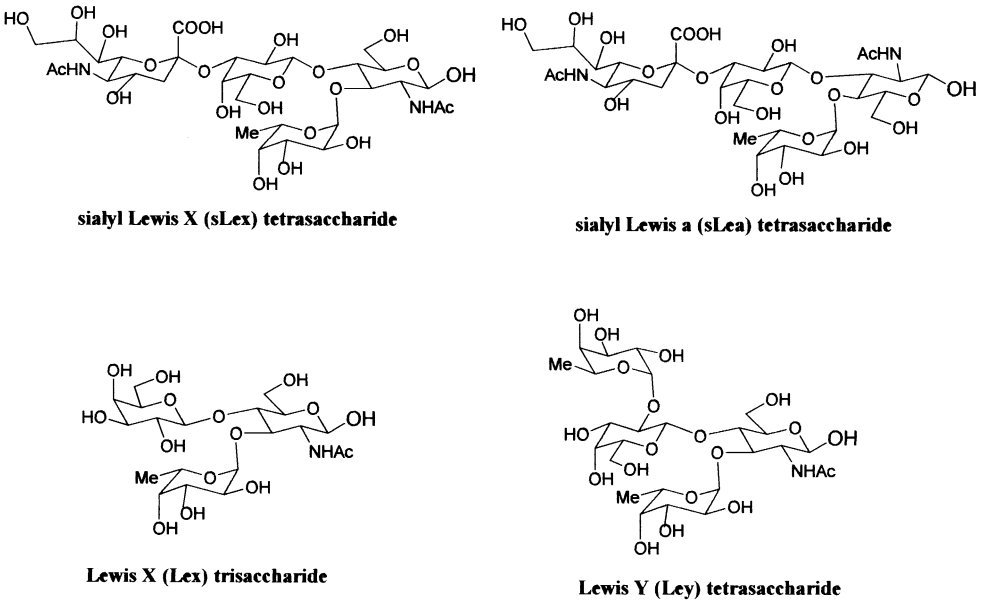

Figure 1. Structures of Lewis Oligosaccharides

drate is known to increase the acidity of boronic acid, the boronic ester formation will also increase the B-N bond strength, which results in the masking of the nitrogen lone pair electrons. Consequently, the fluorescence intensity of the anthracene system increases (Figure 2). Several laboratories, including ours, have used this system developed by the Shinkai group in the synthesis of boronic acid-based fluorescent sensors, for mostly monosaccharides [23–25, 37]. In this project, we also chose to use the Shinkai system as the reporter moiety for the synthesis of diboronic compounds as potential sensors for sLex.

For the construction of fluorescent sensors for sLex, we envisioned that diboronic acid compounds with the proper spatial arrangement of the two boronic acid moieties, which are complementary to the multiple pairs of diols, have the potential for highly specific recognition of the target carbohydrate. Such a concept has been demonstrated several times in the preparation of diboronic acid sensors for glucose and other monosaccharides [23–25, 37]. In this project, we chose to use a spacer to link, through amide bond formation, two fluorescent boronic acid compounds for the synthesis of the potential sensors (**7**, Figure 3). In doing so, we sampled a series of dicarboxylic acid linkers with different length, rigidity, and spatial orientation in search of an optimal arrangement.

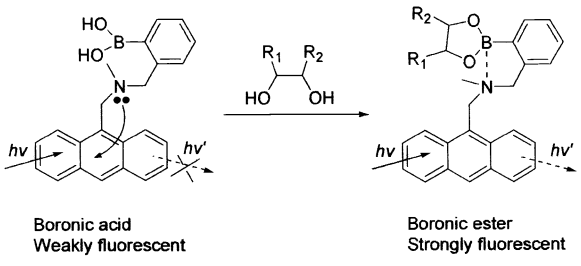

Figure 2. Illustration of the Anthracene-Based Photoinduced Electron Transfer System

The synthesis of these compounds is shown in Figure 3. Starting from the readily available hydroxyaldehyde **1** [38], upon reductive amination with methylamine in MeOH/THF and $NaBH_4$, amine **2** was obtained in 90% yield. The Boc-protected compound **3** was obtained in 78% yield by treatment of **2** with di-*tert*-butyldicarbonate [$(Boc)_2O$] in MeOH in the presence of triethylamine (TEA). This was followed by oxidation with pyridine sulfur trioxide in dimethylsulfoxide (DMSO) in the presence of TEA to give aldehyde **4** in quantitative yield. The resulting aldehyde **4** was then converted to amine compound **5** in 83% yield through reductive amination. Amine **5** was coupled with various diacids using 1-(2-dimethylaminopropyl)-3-ethylcarbodiimide hydrochloride (EDC) as the activating reagent to furnish compounds **6** in 30–90% yields. After deprotection of compounds **6** with trifluoroacetic acid (TFA), the unprotected free amines were then reacted with boronate **8** [23] in the presence of potassium carbonate to give the diboronic acids **7** (Table 1) in 30%–80% yields.

These compounds are designed to show significant fluorescence intensity changes upon binding with a complementary carbohydrate. In screening for their binding with the target carbohydrate, sLex, the fluorescence intensity changes of the sensor solutions upon addition of the carbohydrate were determined. Such experiments were conducted in a mixture of methanol and 0.1 M phosphate buffer (pH 7.4) (1:1, v/v). Methanol was used to improve the solubility of the sensor compounds. The sensor (**7**) concentration was fixed at 1×10^{-5} or 1×10^{-6} M, and the concentration of sLex was set at 60 μM. The fluorescence intensity change profile for these diboronic acids is shown in Figure 4. It can be

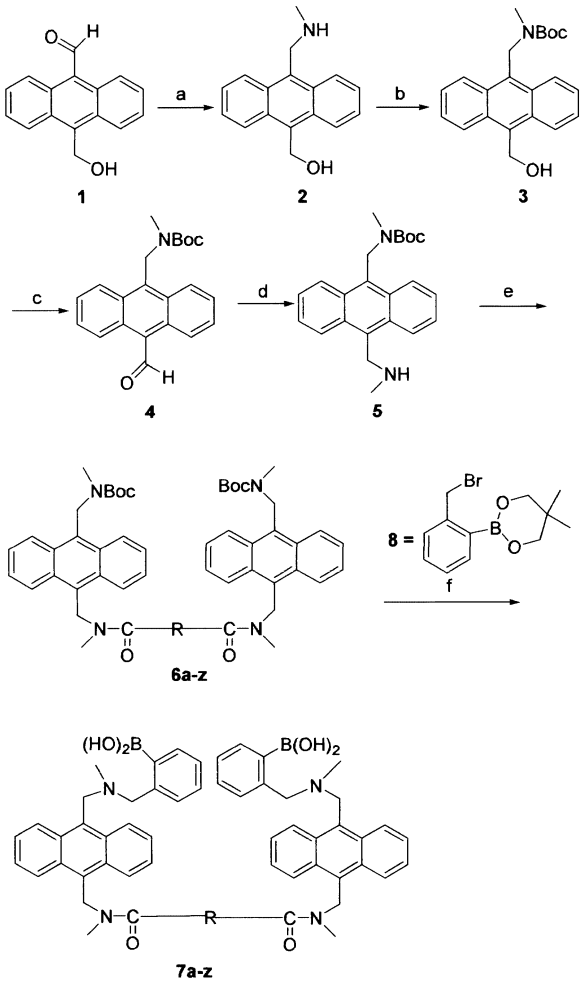

Figure 3. Dibronic Acid Synthesis

(a) i. MeOH, THF, $MeNH_2$ (40%, wt), ii. $NaBH_4$, 90%; (b) MeOH, TEA, $(Boc)_2O$, 78%; (c) DMSO, TEA, $Py{\bullet}SO_3$, 100%; (d) i. MeOH, THF, $MeNH_2$ (40%, wt), ii. $NaBH_4$, 83%. (e) CH_2Cl_2, EDC, HOOCRCOOH, 30–90%; (f) i. TFA, CH_2Cl_2, ii. CH_3CN, **8**, K_2CO_3, 30–80%.

Table 1. Chemical Structures of Diboronic Acids **7a-z**

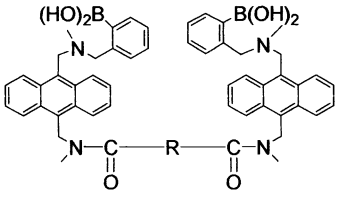

Compounds	R	Compounds	R
7a	$-(CH_2)_{10}-$	**7n**	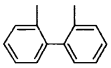
7b		**7o**	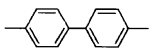
7c	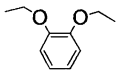	**7p**	$-(CH_2)_5-$
7d	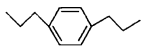	**7q**	
7e	$-(CH_2)_3-$	**7r**	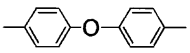
7f		**7s**	
7g		**7t**	
7h	$-(CH_2)_2-$	**7u**	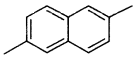
7i	$-(CH_2)_6-$	**7v**	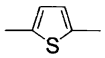
7j	$-(CH_2)_{20}-$	**74**	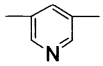
7k		**7x**	$-(CH_2)_{14}-$
7l	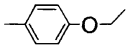	**7y**	$-(CH_2)_4-$
7m	$-(CH_2)_{12}-$	**7z**	

seen that these compounds showed varying degrees of fluorescence intensity changes upon addition of sLex, indicating varying degrees of affinity for the carbohydrate. Among them, compound **7q** showed the greatest fluorescence intensity change upon mixing with sLex.

Biology

Again, our rationale for sensor design targets carbohydrate antigens associated with the development of cancer. Overexpression of sLex in chronic inflammatory diseases of the liver has been reported in several contexts by multiple investigators [15, 16, 39, 40]. Current evidence in our laboratory suggests that sLex serves as a marker for hepatocyte damage and regeneration, and its expression is likely controlled by hepatic cytokines operating in autocrine loops [10–14]. Similarly, Lewis Y appears to be a sensitive marker for damaged intrahepatic bile ducts [40, 41], but its role in the inflammatory process is much less evident. Loss and gain of sLex expression in variously differentiated HCC specimens has been well described [16, 39]. These observations have been linked to the development of cirrhosis, a frequent precursor of HCC. Such findings are comparable to chronic inflammatory states preceding development of colon carcinoma [8]. The specific role(s), if any, for sLex in transformation and progression to HCC are, however, not well understood. Biosensors that could sensitively trace this development in vivo would likely further our understanding of hepatocarcinogenesis, in addition to providing new diagnostic and therapeutic approaches.

After demonstration of binding of the sensors to sLex in solution, it was desirable to see whether **7q,** the compound that showed the most significant fluorescence intensity increase upon addition of sLex, could bind the biomarker sLex on cell surfaces [19, 42]. We therefore chose a cell line that selectively expresses sLex on the

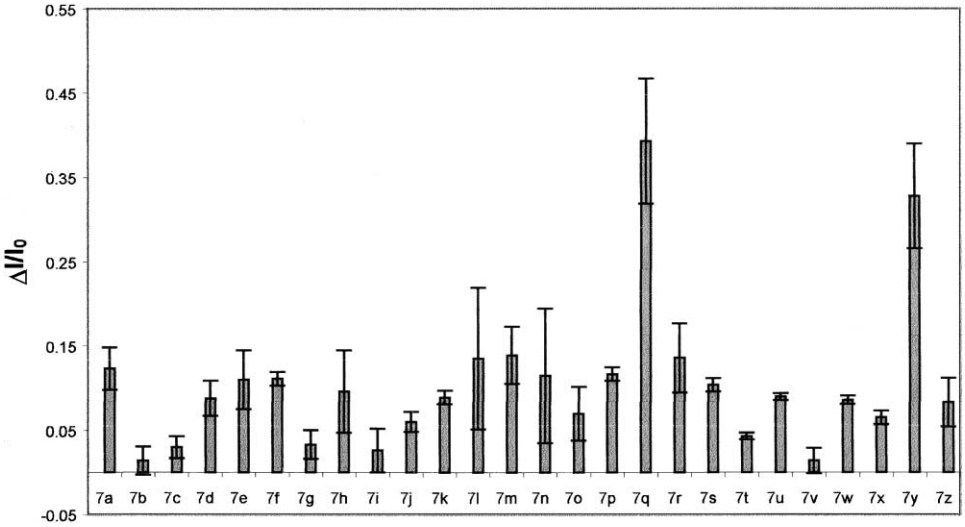

Figure 4. The Fluorescence Intensity Changes of the Diboronic Acids **7a-z** upon Binding with sLex
Sensor concentrations: 1×10^{-5} or 1×10^{-6} M. sLex concentration: 6×10^{-5} M; $\lambda_{ex} = 370$ nm, $\lambda_{em} = 426$ nm.

surface, HEPG2 (Figure 5). To examine the selectivity of the sensor for cell surface sLex, HEP3B and COS7 cells were labeled in parallel. COS7 expresses none of the fucosylated antigens associated with carcinoma progression and HEP3B expresses only the Lewis Y antigen [43, 44]. Flow cytometry analysis of HCC lines with anti-carbohydrate monoclonal antibodies was performed to characterize surface glycan expression. Using two different monoclonal antibodies directed at sLex, HEPG2 cells were found to express high levels, while HEP3B cells expressed little or none (Figure 5). Anti-Lewis Y monoclonal antibodies revealed the converse: high expression on HEP3B and little or no staining of HEPG2. None of the cell lines expressed Lewis X or sialyl Lewis a, related antigens expressed on other forms of carcinoma [9, 19, 42]. These cell lines were then used for the fluorescent labeling studies with the sensors.

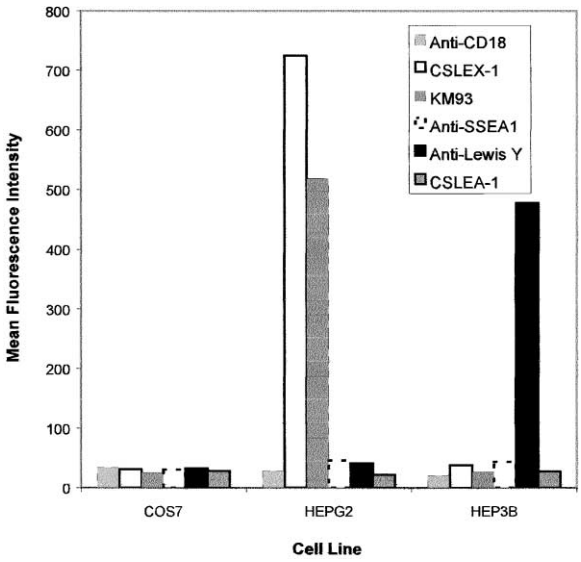

Figure 5. Flow Cytometry Analysis of Surface Antigens on HEPG2, HEP3B, and COS7 Cells

Cells were harvested, stained with monoclonal antibodies, and subjected to flow cytometric analysis as described in experimental procedures. Anti-CD18 results are presented as negative controls. Monoclonal antibodies CSLEX-1 and KM93 both recognize sLex. Data presented here are the representative mean fluorescence intensity values from four experiments. The antigen-positive population of HEPG2 and HEP3B cells was gated at 1.5×10^{1} units, and over 95% of stained cells were identified by these procedures with each primary antibody used.

HEPG2 and control cell lines were incubated with compound **7q** and three other diboronic acids (**7b**, **7d**, **7y**) selected as controls, examined under fluorescent microscopy, and photographed. Images were subjected to densitometry measurement as described in Experimental Procedures. As seen with sLex solution binding studies summarized in Figure 4, Compound **7q** was highest in mean gray value when binding HEPG2 cells expressing sLex (Figure 6). Compound **7q** did not recognize Lewis Y on HEP3B cells. Compound **7b** avidly bound Lewis Y-expressing HEP3B cells, which correlates with solution binding studies using **7b** and Lewis Y (data not shown). Compound **7b** did not recognize sLex on HEPG2 cells at this concentration (1 μM), again correlating with solution binding studies (Figure 4). Even at this relatively low concentration, compound **7y** recognized surface sLex and Lewis Y with equal avidity, concordant with solution binding studies (data not shown). Compound **7d**, which had low affinity for both sLex and Lewis Y in solution, did not label HEPG2 or HEP3B. None of the compounds bound to COS7 cells at any of the concentrations tested. The above results showed that the cell labeling matched well with the solution binding studies using fluorimetry.

Images from a representative cell-labeling experiment are shown in Figure 7. HCC and control cell lines were incubated with compound **7q**, examined under phase contrast and fluorescent microscopy, and digitally photographed as described in Experimental Procedures. As expected, compound **7q** labeled only HEPG2 cells,

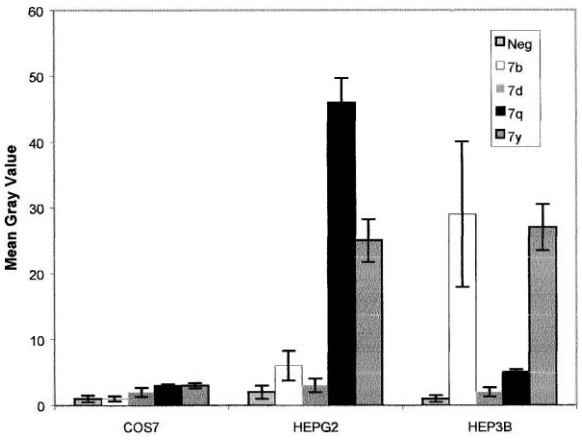

Figure 6. Densitometry Quantification of Fluorescent Compounds Binding to HCC and Control Cell Line

Cells were labeled with 1 μM of sensors **7b**, **7d**, **7y**, and **7q** as described in Experimental Procedures. One well was incubated only in methanol/PBS without compound as a negative control ("neg"). Mean gray values (*y* axis) were determined after subtraction of cell-free background. Results from five experiments are summarized.

exhibiting dose-responsive fluorescence over the range of 0.5–10 μM. Even at higher concentrations, (e.g., 5 μM, Figure 7), **7q** did not recognize Lewis Y on HEP3B cells. We also examined the selectivity of sensor **7b**. Compound **7b** bound Lewis Y-expressing HEP3B cells at all concentrations tested (0.5–10 μM). At higher concentrations, **7b** also labeled HEPG2 cells, suggesting cross-reactivity with sLex (e.g., 5 μM, Figure 7). Thus, sensor **7q** alone appears to have both high sensitivity and specificity for sLex when compared to related compounds and carbohydrate antigens.

To examine whether all components of sLex were essential for binding, HEPG2 cells (sLex-expressing) were treated with neuraminidases specific for α (2,3) sialic acid linkages (MDL number MFCD01092203, SIGMA #N7271) and α (2,3)/α (2,6) sialic acid residues (MDL number MFCD01092201, SIGMA #N5521). Both neuraminidases consistently reduced binding of **7q** by 50%–75% (e.g.; mean gray value of control 69.8 ± 4; mean gray value of N7271-treated 25 ± 9, n = 8 experiments), indicating that sialic acid is required for binding of **7q**. To examine the role of the fucose moiety in **7q** binding, HEPG2 were also incubated with fucosidase recognizing α (1,3)- and (1,4) –linked fucose (MDL number MFCD00130491, SIGMA #F3023). This specific fucosidase reduced **7q** binding by 50%–75% (mean gray value 23.5 ± 11, n = 8 experiments). Fucosidases recognizing other linkages (e.g.; α 1,6, MDL number MFCD01092200, SIGMA #F6272; α 1,2, MDL number MFCD01092199, SIGMA #F9272) had no significant effect on **7q** binding (data not shown). Incubation with both α (1,3/1,4)fucosidase and α (2,3)neuraminidase (same buffers and conditions except pH 5.5) showed almost complete inhibition of **7q** binding (mean gray value less than 10 ± 2 for N7271/F3023-treated cells, n = 4 experiments). Taken together, these results indicate that **7q** likely requires both fucose and sialic acid residues when binding to sLex on cell surfaces.

It is fortuitous that among this first group of diboronic compounds, **7q** was able to label sLex-expressing cells at low concentrations (0.5 μM) without cross-reactivity to Ley-expressing cells (HEP3B). This will serve as an excellent lead compound for further structural optimizations. However, much more work is needed to truly understand the structural features of **7q** that led to this specific labeling activity. Such work will involve extensive computational and conformational work and is beyond the scope of this report.

Significance

Our laboratory has a long-standing interest in the development of small molecule sensors for various analytes. Such sensors can be used for diagnostic purposes. They can also be considered antibody mimics for the high-specificity recognition of cell biomarkers. Antibodies have been used for the development of in vitro diagnostic and detection tools, targeted drug delivery vectors, and tissue-specific imaging agents. However, success in the in vivo application of antibody-based diagnostic and therapeutic agents has been limited partly because of their poor stability, immunogenecity, poor permeability, and complexity in chemical conjugation with the diagnostic or imaging

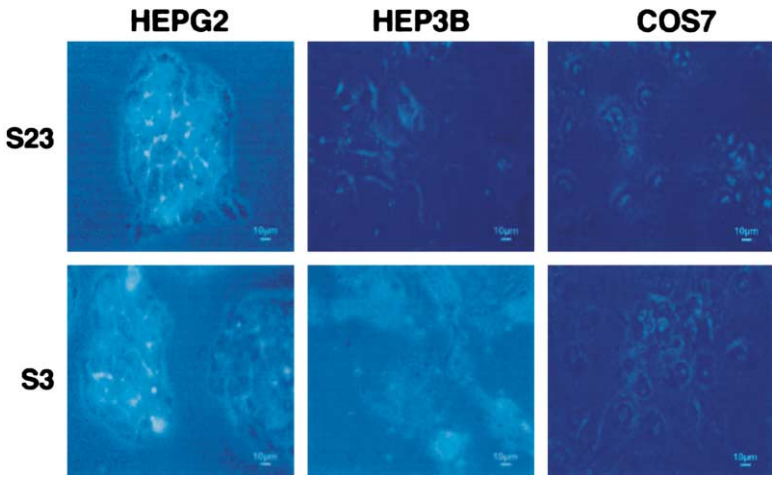

Figure 7. Representative Fluorescent Labeling Studies of HEPG2, HEP3B, and COS7 Cells

HEPG2 cells express only sLex, HEP3B cells express only Lewis Y, and COS7 cells do not express either antigen. Compounds **7q (S-23)** and **7b (S-3)** are used at 5 μM in the examples shown. Excitation wavelength = 370 nm and emission wavelength = 426 nm. Scale in lower right corner indicates 10 μm length.

agents. Small organic molecule-based compounds capable of specific recognition of cell-surface biomarkers can be considered antibody mimics and can be used for the same type of applications. However, the small organic molecule antibody mimics have the advantage of having more desirable pharmaceutical, biopharmaceutical, and chemical properties for the development of pharmaceutical agents. The fluorescent sensor described in this paper represents the first example of a small organic molecule used to fluorescently label cells based on the cell-surface carbohydrate structures. Further development along this line could lead to a number of small molecule antibody mimics that can be used for labeling, drug delivery, and selective imaging applications.

Experimental Procedures

Chemistry

General

All ^1H and ^{13}C NMR spectra were recorded at 300 MHz and 75 MHz, respectively, with tetramethylsilane as the internal standard. Column chromatography was performed using silica gel (200-400 mesh) from Aldrich and neutral activated Brockmann I aluminum oxide (~150 mesh) from EM Science. Elemental analyses were performed by Atlantic Microlab, Inc., Norcross, GA. Mass spectral analyses were performed by the North Carolina State University Mass Spectrometry Facility and the University of Kansas Mass Spectrometry Laboratory. IR spectra were recorded on a Perkin-Elmer 1600 series spectrometer. Tetrahydrofuran (THF) was distilled from Na and benzophenone. Acetonitrile (CH_3CN) and dichloromethane (CH_2Cl_2) were distilled from CaH_2. All pH values were determined with an Accumet 1003 Handhold pH/mV/Ion Meter (Fisher Scientific). A Shimadzu RF-5301 PC fluorimeter was used for the fluorescence studies. The excitation wavelength was set at 370 nm.

(10-Methylaminomethyl-anthracen-9-yl)-methanol (2)

To the solution of compound **1** (2.00 g, 8.47 mmol) in MeOH (100 mL) and THF (50 mL) was added the aqueous solution of methylamine (40%, wt, 20 mL). The resulting mixture was stirred at room temperature under nitrogen for 16 hr and then sodium borohydride (0.90 g, 23.7 mmol) was added and the mixture stirred for another 30 min. After solvent evaporation, the resulting solid was dissolved in the mixture of ethyl acetate (100 mL) and water (50 mL). The organic phase was separated and dried over $MgSO_4$. Solvent evaporation gave a crude product, which was purified on a silica gel column, eluting with $MeOH/CH_2Cl_2$ (1/50), to give compound **2** as a yellow solid (1.91 g, 90%). ^1H NMR ($CDCl_3$) δ 8.45–8.42 (m, 2H), 8.37–8.34 (m, 2H), 7.55–7.52 (m, 4H), 5.64 (s, 2H), 4.65 (s, 2H), 2.65 (s, 3H). ^{13}C NMR ($CDCl_3$) δ 133.4, 131.7, 130.4, 130.3, 126.2, 126.1, 125.1, 124.8, 57.7, 48.2, 37.3. HRMS (FAB) calculated for $C_{17}H_{18}NO$ ($M^+ + H$) 252.1388, found 252.1373. Elemental analysis calculated for $C_{17}H_{17}NO$: C, 81.24; H, 6.82; N, 5.57. Found: C, 80.96; H, 6.86; N, 5.53.

(10-Hydroxymethyl-anthracen-9-ylmethyl)-methyl-carbamic acid tert-butyl ester (3)

Compound **2** (2.10 g, 8.37 mmol), di-*tert*-butyl dicarbonate (3.80 g, 17.4 mmol), and trimethylamine (20 mL) were mixed in MeOH (120 mL) and then stirred at room temperature for 30 min. After removal of the solvent, the resulting residue was dissolved in ethyl acetate (100 mL), washed with water (3 × 50 mL), 10% aqueous solution of sodium carbonate (30 mL), and saturated brine (50 mL) and dried over $MgSO_4$. Solvent evaporation gave a crude product, which was purified on a silica gel column, eluting with ethyl acetate/hexanes (1/50–1/2), giving compound **3** as a yellow solid (2.30 g, 78%). ^1H NMR ($CDCl_3$) δ 8.51–8.43 (m, 4H), 7.60–7.55 (m, 4H), 5.71 (d, J = 5.6 Hz, 2H), 5.50 (s, 2H), 2.47 (s, 3H), 1.55 (s, 9H). ^{13}C NMR ($CDCl_3$) δ 156.0, 132.6, 131.3, 130.2, 129.9, 126.1, 125.8, 125.4, 125.0, 80.1, 57.6, 42.7, 31.8, 28.7. IR (cm^{-1}): 3413, 1681. HRMS (FAB) calculated for $C_{22}H_{25}NO_3$ (M^+) 351.1834, found 351.1835. Elemental analysis calculated for $C_{22}H_{25}NO_3$: C, 75.19; H, 7.17; N, 3.99. Found: C, 75.21; H, 7.27; N, 3.97.

(10-Formyl-anthracen-9-ylmethyl)-methyl-carbamic acid tert-butyl ester (4)

Compound **3** (2.30 g, 6.55 mmol) was dissolved in the mixture of dry DMSO (20 mL) and trimethylamine (20 mL). To the solution thus prepared was added the solution of pyridine sulfur trioxide (7.30 g, 45.9 mmol) dissolved in dry DMSO (20 mL) over a period of 30 min. The reaction mixture was stirred at room temperature under nitrogen for 30 min, and then poured into ice-water (300 mL), extracted with ethyl acetate (3 × 100 mL), dried over $MgSO_4$. Solvent evaporation gave a yellow solid (2.30 g, 100%) without further purification. ^1H NMR ($CDCl_3$) δ 11.51 (s, 1H), 8.90 (d, J = 8.5 Hz, 2H), 8.51 (d, J = 8.5 Hz, 2H), 7.70–7.61 (m, 4H), 5.56 (s, 2H), 2.48 (s, 3H), 1.56 (s, 9H).

Methyl-(10-methylaminomethyl-anthracen-9-ylmethyl)-carbamic acid tert-butyl ester (5)

Compound **4** (2.29 g, 6.56 mmol) was dissolved in the mixture of THF (50 mL) and MeOH (50 mL). To this solution was added the aqueous solution of methylamine (40%, wt, 20 mL), the reaction mixture was stirred at room temperature under nitrogen for 12 hr. Sodium borohydride (1.00 g, 26.3 mmol) was added, and stirred for 30 min. After removal of the solvent in vacuo, the resulting residue was dissolved in ethyl acetate (100 mL), washed with water (3 × 50 mL), and dried over $MgSO_4$. Solvent evaporation gave a crude product, which was purified on a silica gel column, eluting with $MeOH/CH_2Cl_2$ (1/2), giving compound **5** as a yellow solid (2.00 g, 83%). ^1H NMR ($CDCl_3$) δ 8.44–8.39 (m, 4H), 7.56–7.53 (m, 4H), 5.51 (s, 2H), 4.71 (s, 2H), 2.69 (s, 3H), 2.46 (s, 3H), 1.55 (s, 9H). ^{13}C NMR ($CDCl_3$) δ 155.6, 132.5, 131.0, 130.0, 125.8, 125.7, 125.4, 125.3, 124.9, 79.7, 47.8, 42.6, 36.9, 31.6, 28.6. IR (cm^{-1}): 1686. HRMS (FAB) calculated for $C_{23}H_{28}N_2O_2$ (M^+) 364.2151, found 364.2159. Elemental analysis calculated for $C_{23}H_{28}N_2O_2$: C, 75.79; H, 7.74; N, 7.69. Found: C, 75.64; H, 7.71; N, 7.53.

General Procedures for Preparation of Boc-Protected Diamines (6)

The di-acid (0.138 mmol, 0.5 equivalent) was dissolved in dry CH_2Cl_2 (20 mL), then 1-(2-dimethylaminopropyl)-3-ethylcarbodiimide hydrochloride (EDC, 210 mg, 1.10 mmol, 4.0 equivalent) was added. To this solution was added compound **5** (100 mg, 0.275 mmol, 1.0 equivalent). The reaction mixture was stirred at room temperature under nitrogen for 12 hr, then washed with water (2 × 30 mL) and dried over $MgSO_4$. After solvent evaporation, the crude product was purified on a silica gel column, eluting with $MeOH/CH_2Cl_2$ to give the product.

[10-({[11-({10-[(Tert-Butoxycarbonyl-methyl-amino)-methyl]-anthracen-9-ylmethyl}-methyl-carbamoyl)-undecanoyl]-methyl-amino}-methyl)-anthracen-9-ylmethyl]-methyl-carbamic acid tert-butyl ester (6a)

Yield 52%. ^1H NMR ($CDCl_3$) δ 8.49–8.46 (m, 4H), 8.40–8.37 (m, 4H), 7.59–7.54 (m, 8H), 5.71 (s, 4H), 5.54 (s, 4H), 2.60 (s, 6H), 2.49 (s, 6H), 2.40–2.35 (m, 4H), 1.72–1.55 (m, 22H), 1.36–1.31 (m, 12H). IR (cm^{-1}): 1684, 1637. HRMS (FAB) calculated for $C_{58}H_{75}N_4O_6$ ($M^+ + H$) 923.5687, found 923.5716.

(10-{[(2-{2-[({10-[(Tert-Butoxycarbonyl-methyl-amino)-methyl]-anthracen-9-ylmethyl}-methyl-carbamoyl)-methyl]-phenyl-acetyl)-methyl-amino]-methyl}-anthracen-9-ylmethyl)-methyl-carbamic acid tert-butyl ester (6b)

Yield 88%. ^1H NMR ($CDCl_3$) δ 8.47–8.39 (m, 8H), 7.53–7.49 (m, 8H), 7.26 (d, J = 4.2 Hz, 4H), 5.74 (s, 4H), 5.53 (s, 4H), 3.81 (s, 4H), 2.62 (s, 6H), 2.45 (s, 6H), 1.56 (s, 18H). IR (cm^{-1}): 1684, 1643. HRMS (FAB) calculated for $C_{56}H_{63}N_4O_6$ ($M^+ + H$) 887.4748, found 887.4733.

10-{[(2-{2-[({10-[(Tert-Butoxycarbonyl-methyl-amino)-methyl]-anthracen-9-ylmethyl}-methyl-carbamoyl)-methoxy]-phenoxy}-acetyl)-methyl-amino]-methyl}-anthracen-9-ylmethyl)-methyl-carbamic acid tert-butyl ester (6c)

Yield 44%. ^1H NMR ($CDCl_3$) δ 8.47 (d, J = 9.0 Hz, 4H), 8.33 (d, J = 9.0 Hz, 4H), 7.54–7.49 (m, 8H), 7.0 (s, 4H), 5.69 (s, 4H), 5.51 (s, 4H), 4.79 (s, 4H), 2.60 (s, 6H), 2.47 (s, 6H), 1.60 (s, 18H). IR (cm^{-1}): 1672. HRMS (FAB) calculated for $C_{56}H_{63}N_4O_8$ ($M^+ + H$) 919.4646, found 919.4681.

(10-{[(3-{4-[2-({10-[(Tert-Butoxycarbonyl-methyl-amino)-methyl]-anthracen-9-ylmethyl}-methyl-carbamoyl)-ethyl]-phenyl}-propionyl)-methyl-amino]-methyl}-anthracen-9-ylmethyl)-methyl-carbamic acid tert-butyl ester (6d)

Yield 73%. ^1H NMR ($CDCl_3$) δ 8.48–8.45 (m, 4H), 8.38–8.35 (m, 4H), 7.57–7.54 (m, 8H), 7.18 (s, 4H), 5.71 (s, 4H), 5.53 (s, 4H), 3.06 (t, J =

8.7 Hz, 4H), 2.65 (t, J = 8.7 Hz, 4H), 2.53 (s, 6H), 2.48 (s, 6H), 1.56 (s, 18H). IR (cm^{-1}): 1684, 1643. HRMS (FAB) calculated for $C_{58}H_{67}N_4O_6$ (M^+ + H) 915.5061 found 915.5070.

[10-({[4-({10-[(Tert-Butoxycarbonyl-methyl-amino)-methyl]-anthracen-9-ylmethyl}-methyl-carbamoyl)-butyryl]-methyl-amino}-methyl)-anthracen-9-ylmethyl]-methyl-carbamic acid tert-butyl ester (6e)

Yield 53%. ^1H NMR ($CDCl_3$) δ 8.48–8.45 (m, 4H), 8.39–8.35 (m, 4H), 7.55–7.52 (m, 8H), 5.69 (s, 4H), 5.54 (s, 4H), 2.63 (s, 6H), 2.54 (t, J = 7.0 Hz, 4H), 2.48 (s, 6H), 2.20–2.10 (m, 2H), 1.57 (s, 18H). IR (cm^{-1}): 1685, 1639. HRMS (FAB) calculated for $C_{51}H_{61}N_4O_6$ (M^+ + H) 825.4591, found 825.4627. Elemental analysis calculated for $C_{51}H_{60}N_4O_6 \cdot 1.5H_2O$: C, 71.82; H, 7.39; N, 6.57. Found: C, 71.93; H, 7.43; N, 6.27.

[10-({[2-({10-[(Tert-Butoxycarbonyl-methyl-amino)-methyl]-anthracen-9-ylmethyl}-methyl-carbamoyl)-benzoyl]-methyl-amino}-methyl)-anthracen-9-ylmethyl]-methyl-carbamic acid tert-butyl ester (6f)

Yield 64%. ^1H NMR ($CDCl_3$) δ 8.58–8.51 (m, 8H), 7.67–7.60 (m, 8H), 7.29–7.26 (m, 2H), 7.08 (m, 2H), 5.94 (s, 4H), 5.58 (s, 4H), 2.67 (s, 6H), 2.53 (s, 6H), 1.57 (s, 18H). IR (cm^{-1}): 1680, 1633. HRMS (FAB) calculated for $C_{54}H_{59}N_4O_6$ (M^+ + H) 859.4435, found 859.4449. Elemental analysis calculated for $C_{54}H_{58}N_4O_6 \cdot 1.5H_2O$: C, 73.13; H, 6.88; N, 6.32. Found: C, 73.02; H, 6.68; N, 6.21.

[10-({[5-({10-[(Tert-Butoxycarbonyl-methyl-amino)-methyl]-anthracen-9-ylmethyl}-methyl-carbamoyl)-pent-3-enoyl]-methyl-amino}-methyl)-anthracen-9-ylmethyl]-methyl-carbamic acid tert-butyl ester (6g)

Yield 31%. ^1H NMR ($CDCl_3$) δ 8.46–8.43 (m, 4H), 8.36–8.32 (m, 4H), 7.59–7.56 (m, 8H), 5.79 (s, 2H), 5.68 (s, 4H), 5.52 (s, 4H), 3.24 (s, 4H), 2.56 (s, 6H), 2.48 (s, 6H), 1.56 (s, 18H). IR (cm^{-1}): 1689, 1642. HRMS (FAB) calculated for $C_{52}H_{61}N_4O_6$ (M^+ + H) 837.4591, found 837.4592. Elemental analysis calculated for $C_{52}H_{60}N_4O_6 \cdot 2\,H_2O$: C, 71.55; H, 7.33; N, 6.42. Found: C, 71.70; H, 7.03; N, 6.31.

[10-({[3-({10-[(Tert-Butoxycarbonyl-methyl-amino)-methyl]-anthracen-9-ylmethyl}-methyl-carbamoyl)-propionyl]-methyl-amino}-methyl)-anthracen-9-ylmethyl]-methyl-carbamic acid tert-butyl ester (6h)

Yield 78%. ^1H NMR ($CDCl_3$) δ 8.48–8.41 (m, 8H), 7.60–7.55 (m, 8H), 5.77 (s, 4H), 5.56 (s, 4H), 2.86 (s, 4H), 2.79 (s, 6H), 2.50 (s, 6H), 1.53 (s, 18H). IR (cm^{-1}): 1685, 1643. HRMS (FAB) calculated for $C_{50}H_{59}N_4O_6$ (M^+ + H) 811.4356, found 811.4412. Elemental analysis calculated for $C_{50}H_{58}N_4O_6$: C, 74.05; H, 7.21; N, 6.91. Found: C, 74.01; H, 7.34; N, 6.63.

[10-({[7-({10-[(Tert-Butoxycarbonyl-methyl-amino)-methyl]-anthracen-9-ylmethyl}-methyl-carbamoyl)-heptanoyl]-methyl-amino}-methyl)-anthracen-9-ylmethyl]-methyl-carbamic acid tert-butyl ester (6i)

Yield 75%. ^1H NMR ($CDCl_3$) δ 8.49–8.38 (m, 8H), 7.58–7.55 (m, 8H), 5.71 (s, 4H), 5.54 (s, 4H), 2.60 (s, 6H), 2.50 (s, 6H), 2.39 (t, J = 1.5 Hz, 4H), 1.90–1.40 (m, 8H), 1.58 (s, 18H). IR (cm^{-1}): 1684, 1636. HRMS (FAB) calculated for $C_{54}H_{69}N_4O_6$ (M^+ + H) 867.4982, found 867.5229.

[10-({[21-({10-[(Tert-Butoxycarbonyl-methyl-amino)-methyl]-anthracen-9-ylmethyl}-methyl-carbamoyl)-heneicosanoyl]-methyl-amino}-methyl)-anthracen-9-ylmethyl]-methyl-carbamic acid tert-butyl ester (6j)

Yield 64%. ^1H NMR ($CDCl_3$) δ 8.49–8.38 (m, 8H), 7.59–7.56 (m, 8H), 5.72 (s, 4H), 5.55 (s, 4H), 2.60 (s, 6H), 2.50 (s, 6H), 2.40–2.34 (m, 4H), 1.90–1.20 (m, 54H). IR (cm^{-1}): 1692, 1643. HRMS (FAB) calculated for $C_{68}H_{95}N_4O_6$ (M^+ + H), 1063.7173, found 1063.5746. Elemental analysis calculated for $C_{54}H_{58}N_4O_6 \cdot 0.5H_2O$: C, 72.15; H, 8.92; N, 5.22. Found: C, 76.15; H, 8.92; N, 4.76.

[10-({[3-({10-[(Tert-Butoxycarbonyl-methyl-amino)-methyl]-anthracen-9-ylmethyl}-methyl-carbamoyl)-benzoyl]-methyl-amino}-methyl)-anthracen-9-ylmethyl]-methyl-carbamic acid tert-butyl ester (6k)

Yield 74%. ^1H NMR ($CDCl_3$) δ 8.52–8.45 (m, 8H), 7.60–7.56 (m, 8H), 7.50–7.40 (m, 4H), 5.85 (s, 4H), 5.58 (s, 4H), 2.53 (s, 12H), 1.59 (s, 18H). IR (cm^{-1}): 1688, 1632. HRMS (FAB) calculated for $C_{54}H_{59}N_4O_6$ (M^+ + H) 859.4435, found 859.4832. Elemental analysis calculated for $C_{54}H_{58}N_4O_6 \cdot 1.5H_2O$: C, 73.20; H, 6.88; N, 6.32. Found: C, 73.46; H, 6.93; N, 6.05.

{10-[({4-[({10-[(Isopropoxycarbonyl-methyl-amino)-methyl]-anthracen-9-ylmethyl}-methyl-carbamoyl)-methoxy]-benzoyl}-methyl-amino)-methyl]-anthracen-9-ylmethyl}-methyl-carbamic acid tert-butyl ester (6l)

Yield 60%. ^1H NMR ($CDCl_3$) δ 8.50–8.31 (m, 8H), 7.62–7.43 (m, 10H), 6.99–6.96 (m, 2H), 5.86 (s, 2H), 5.72 (s, 2H), 5.58–5.54 (m, 4H), 4.79 (s, 2H), 2.65 (s, 3H), 2.62 (s, 3H), 2.53 (s, 3H), 2.49 (s, 3H), 1.58 (s, 18H). IR (cm^{-1}): 1682, 1626. HRMS (FAB) calculated for $C_{55}H_{61}N_4O_7$ (M^+ + H) 889.4462, found 889.4086. Elemental analysis calculated for $C_{52}H_{60}N_4O_7 \cdot H_2O$: C, 73.56; H, 6.85; N, 6.23. Found: C, 73.31; H, 7.50; N, 5.35.

[10-({[13-({10-[(Tert-Butoxycarbonyl-methyl-amino)-methyl]-anthracen-9-ylmethyl}-methyl-carbamoyl)-tridecanoyl]-methyl-amino}-methyl)-anthracen-9-ylmethyl]-methyl-carbamic acid tert-butyl ester (6m)

Yield 52%. ^1H NMR ($CDCl_3$) δ 8.60–8.36 (m, 8H), 7.64–7.46 (m, 8H), 5.72 (s, 4H), 5.55 (s, 4H), 2.60 (s, 6H), 2.50 (s, 6H), 2.42–2.32 (m, 4H), 1.92–1.20 (m, 20H), 1.56 (s, 18H). HRMS (FAB) calculated for $C_{60}H_{79}N_4O_6$ (M^+ + H) 951.6000, found 951.6009. Elemental analysis calculated. for $C_{60}H_{78}N_4O_6$: C, 75.75; H, 8.26; N, 5.89. Found: C, 75.55; H, 8.37; N, 5.75.

[10-({[2′-({10-[(Tert-Butoxycarbonyl-methyl-amino)-methyl]-anthracen-9-ylmethyl}-methyl-carbamoyl)-biphenyl-2-carbonyl]-methyl-amino}-methyl)-anthracen-9-ylmethyl]-methyl-carbamic acid tert-butyl ester (6n)

Yield 59%. ^1H NMR ($CDCl_3$) δ 8.54–8.20 (m, 8H), 7.64–7.44 (m, 8H), 7.42–7.20 (m, 8H), 5.51 (s, 8H), 5.51 (s, 8H), 2.47 (s, 12H), 1.57 (s, 18H). HRMS (FAB) calculated for $C_{60}H_{63}N_4O_6$ (M^+ + H) 935.4748, found 935.4770. Elemental analysis calculated. for $C_{60}H_{62}N_4O_6 \cdot 0.5H_2O$: C, 76.32; H, 6.72; N, 5.93. Found: C, 76.57; H, 7.09; N, 5.65.

[10-({[4′-({10-[(Tert-Butoxycarbonyl-methyl-amino)-methyl]-anthracen-9-ylmethyl}-methyl-carbamoyl)-biphenyl-4-carbonyl]-methyl-amino}-methyl)-anthracen-9-ylmethyl]-methyl-carbamic acid tert-butyl ester (6o)

Yield 62%. ^1H NMR ($CDCl_3$) δ 8.40–8.20 (m, 8H), 7.80–7.40 (m, 16H), 5.90 (s, 4H), 5.57 (s, 4H), 2.60 (s, 6H), 2.52 (s, 6H), 1.58 (s, 18H). HRMS (FAB) calculated for $C_{60}H_{63}N_4O_6$ (M^+ + H) 935.4748, found 935.4775. Elemental analysis calculated. for $C_{60}H_{62}N_4O_6 \cdot 0.5H_2O$: C, 76.32; H, 6.72; N, 5.93. Found: C, 76.29; H, 6.68; N, 5.94.

[10-({[6-({10-[(Tert-Butoxycarbonyl-methyl-amino)-methyl]-anthracen-9-ylmethyl}-methyl-carbamoyl)-hexanoyl]-methyl-amino}-methyl)-anthracen-9-ylmethyl]-methyl-carbamic acid tert-butyl ester (6p)

Yield 56%. ^1H NMR ($CDCl_3$) δ 8.52–8.36 (m, 8H), 7.64–7.54 (m, 8H), 5.71 (s, 4H), 5.54 (s, 4H), 2.60 (s, 6H), 2.49 (s, 6H), 2.41 (t, J = 7.5 Hz, 4H), 1.90–1.20 (m, 6H), 1.57 (s, 18H). IR (cm^{-1}): 1683, 1635. HRMS (FAB) calculated for $C_{53}H_{65}N_4O_6$ (M^+ + H) 853.4904; found 853.4916.

[10-({[4-({10-[(Tert-Butoxycarbonyl-methyl-amino)-methyl]-anthracen-9-ylmethyl}-methyl-carbamoyl)-benzoyl]-methyl-amino}-methyl)-anthracen-9-ylmethyl]-methyl-carbamic acid tert-butyl ester (6q)

Yield 57%. ^1H NMR ($CDCl_3$) δ 8.60–8.40 (m, 8H), 7.63–7.55 (m, 8H), 7.40 (s, 4H), 5.86 (s, 4H), 5.55 (s, 4H), 2.51 (s, 12H), 1.62 (s, 18H). IR (cm^{-1}): 1684, 1635. HRMS (FAB) calculated for $C_{54}H_{59}N_4O_6$ (M^+ + H) 859.4435; found 859.4451.

{10-[({4-[4-({10-[(Tert-Butoxycarbonyl-methyl-amino)-methyl]-anthracen-9-ylmethyl}-methyl-carbamoyl)-phenoxy]-benzoyl}-methyl-amino)-methyl]-anthracen-9-ylmethyl}-methyl-carbamic acid tert-butyl ester (6r)

Yield 79%. ^1H NMR ($CDCl_3$) δ 8.60–8.40 (m, 8H), 7.70–7.50 (m, 8H), 7.49–7.39 (m, 4H), 7.09–6.99 (m, 4H), 5.84 (s, 4H), 5.55 (s, 4H), 2.58 (s, 6H), 2.40 (s, 6H), 1.57 (s, 18H). IR (cm^{-1}): 1682, 1632. HRMS (FAB) calculated for $C_{60}H_{63}N_4O_7$ (M^+ + H) 951.4697; found 951.4684.

[10-({[4-({10-[(Tert-Butoxycarbonyl-methyl-amino)-methyl]-anthracen-9-ylmethyl}-methyl-carbamoyl)-cyclohexanecarbonyl]-methyl-amino}-methyl)-anthracen-9-ylmethyl]-methyl-carbamic acid tert-butyl ester (6s)

Yield 83%. ^1H NMR ($CDCl_3$) δ 8.60–8.40 (m, 4H), 8.38–7.22 (m, 4H), 7.70–7.50 (m, 8H), 5.72 (s, 4H), 5.55 (s, 4H), 2.66 (s, 6H), 2.45 (s, 6H), 1.90–1.86 (m, 4H), 1.77–1.50 (m, 4H), 1.55 (s, 18H). IR (cm^{-1}): 1682, 1634. HRMS (FAB) calculated for $C_{54}H_{63}N_4O_6$ (M^+ + H) 865.4904; found 865.4886.

[10-({[4-({10-[(Tert-Butoxycarbonyl-methyl-amino)-methyl]-anthracen-9-ylmethyl}-methyl-carbamoyl)-cyclohexanecarbonyl]-methyl-amino}-methyl)-anthracen-9-ylmethyl]-methyl-carbamic acid tert-butyl ester (6t)

Yield 83%. ^1H NMR ($CDCl_3$) δ 8.60–8.40 (m, 8H), 7.70–7.50 (m, 8H), 5.77 (s, 4H), 5.56 (s, 4H), 2.70 (s, 6H), 2.55 (s, 6H), 2.56–2.22 (m, 4H), 1.48 (s, 18H), 1.40–1.20 (m, 4H). IR (cm^{-1}): 1686, 1637. HRMS (FAB) calculated for $C_{54}H_{65}N_4O_6$ (M^+ + H) 865.4904; found 865.4886.

[10-({[6-({10-[(Tert-Butoxycarbonyl-methyl-amino)-methyl]-anthracen-9-ylmethyl}-methyl-carbamoyl)-naphthalene-2-carbonyl]-methyl-amino}-methyl)-anthracen-9-ylmethyl]-methyl-carbamic acid tert-butyl ester (6u)

Yield 67%. ^{1}H NMR ($CDCl_3$) δ 8.53–8.50 (m, 8H), 7.89–7.86 (m, 4H), 7.62–7.51 (m, 10H), 5.91 (s, 4H), 5.56 (s, 4H), 2.59 (s, 6H), 2.51 (s, 6H), 1.57 (s, 18H). IR (cm^{-1}): 1688, 1631. MS-FAB 909.8 ($M^+ + H$).

[10-({[5-({10-[(Tert-Butoxycarbonyl-methyl-amino)-methyl]-anthracen-9-ylmethyl}-methyl-carbamoyl)-thiophene-2-carbonyl]-methyl-amino}-methyl)-anthracen-9-ylmethyl]-methyl-carbamic acid tert-butyl ester (6v)

Yield 55%. ^{1}H NMR ($CDCl_3$) δ 8.52–8.49 (m, 4H), 8.39–8.37 (m, 4H), 7.61–7.56 (m, 8H), 7.24 (s, 2H), 5.86 (s, 4H), 5.56 (s, 4H), 2.80 (s, 6H), 2.51 (s, 6H), 1.56 (s, 18H). IR (cm^{-1}): 1686, 1612. HRMS (FAB) calculated for $C_{52}H_{57}N_4O_6S$ ($M^+ + H$) 865.3999, found 865.3973.

[10-({[5-({10-[(Tert-Butoxycarbonyl-methyl-amino)-methyl]-anthracen-9-ylmethyl}-methyl-carbamoyl)-pyridine-3-carbonyl]-methyl-amino}-methyl)-anthracen-9-ylmethyl]-methyl-carbamic acid tert-butyl ester (6w)

Yield 69%. ^{1}H NMR ($CDCl_3$) δ 8.64 (s, 2H), 8.55–8.52 (m, 4H), 8.43–8.41 (m, 4H), 7.85 (s, 1H), 7.62–7.59 (m, 8H), 5.87 (s, 4H), 5.58 (s, 4H), 2.58 (s, 6H), 2.52 (s, 6H), 1.58 (s, 18H). IR (cm^{-1}): 1682, 1632. HRMS (FAB) calculated for $C_{53}H_{58}N_5O_6$ (M^+) 860.4387, found 860.4412.

[10-({[15-({10-[(Tert-Butoxycarbonyl-methyl-amino)-methyl]-anthracen-9-ylmethyl}-methyl-carbamoyl)-pentadecanoyl]-methyl-amino}-methyl)-anthracen-9-ylmethyl]-methyl-carbamic acid tert-butyl ester (6x)

Yield 63%. ^{1}H NMR ($CDCl_3$) δ 8.52–8.49 (m, 4H), 8.43–8.40 (m, 4H), 7.61–7.58 (m, 8H), 5.74 (s, 4H), 5.57 (s, 4H), 2.62 (s, 6H), 2.52 (s, 6H), 2.40 (t, J = 7.2 Hz, 4H), 1.75–1.58 (m, 22H), 1.36–1.29 (m, 20H). IR (cm^{-1}): 1688, 1641. HRMS (FAB) calculated for $C_{62}H_{83}N_4O_6$ ($M^+ + H$) 979.6313, found 979.6343.

[10-({[5-({10-[(Tert-Butoxycarbonyl-methyl-amino)-methyl]-anthracen-9-ylmethyl}-methyl-carbamol)-pentanoyl]-methyl-amino}-methyl)-anthracen-9-ylmethyl]-methyl-carbamic acid tert-butyl ester (6y)

Yield 50%. ^{1}H NMR ($CDCl_3$) δ 8.50–8.30 (m, 8H), 7.60–7.40 (m, 8H), 5.72 (s, 4H), 5.51 (s, 4H), 2.55 (s, 6H), 2.50 (s, 6H), 2.50–2.44 (m, 4H), 1.90–1.60 (m, 4H), 1.57 (s, 18H).

[10-({[4-({10-[(Tert-Butoxycarbonyl-methyl-amino)-methyl]-anthracen-9-ylmethyl}-methyl-carbamoyl)-naphthalene-1-carbonyl]-methyl-amino}-methyl)-anthracen-9-ylmethyl]-methyl-carbamic acid tert-butyl ester (6z)

Yield 33%. ^{1}H NMR ($CDCl_3$) d 8.80-8.40 (m, 8H), 8.00-7.40 (m, 14H), 6.10 (s, 4H), 5.65 (s, 4H), 2.60 (s, 6H), 2.40 (s, 6H), 1.60 (s, 18H). HRMS (FAB) calculated for $C_{58}H_{61}N_4O_6$ ($M^+ + H$) 909.4591, found 909.4583. Elemental analysis calculated. for $C_{58}H_{60}N_4O_6$: C, 76.63; H, 6.65; N, 6.16. Found: C, 76.36; H, 6.72; N, 6.04.

General Procedures for Preparation of the Symmetrical Diboronic Acids (7)

The Boc-protected diamine compound **6** (0.073 mmol) was dissolved in dry CH_2Cl_2 (8mL), then trifluoroacetic acid (3 mL) was added. After the mixture was stirred at room temperature for 10 min, the solvent was removed. The residue was dried in vacuo for 3 hr and dissolved in dry acetonitrile (30 mL); compound **8** (85 mg, 0.30 mmol), potassium carbonate (100 mg, 0.73 mmol) and potassium iodide (2 mg) were then added. The reaction mixture was stirred at room temperature for 12 hr. The insoluble materials were filtered off, and the filtrate was evaporated in vacuo. The resulting residue was dissolved in CH_2Cl_2 and 10% aqueous solution of sodium bicarbonate (20 mL) and the mixture was stirred at room temperature for 1 hr. The organic phase was separated and washed with water (2 × 30 mL) and dried over $MgSO_4$. After removal of the solvent, the crystalline was precipitated from CH_2Cl_2/Et_2O.

Diboronic Acid 7a

Yield 49%. ^{1}H NMR (CD_3OD) δ 8.46–8.43 (m, 4H), 8.29–8.24 (m, 4H), 7.70–7.67 (m, 2H), 7.59–7.55 (m, 8H), 7.36–7.26 (m, 6H), 5.68 (s, 4H), 5.06 (s, 4H), 4.36 (s, 4H), 2.58 (s, 6H), 2.43–2.38 (m, 4H), 1.64–1.54 (m, 4H), 1.36–1.28 (m, 12H). IR (cm^{-1}): 1637. MS-ESI: 496.4 ($M^+ + 2H$)/2.

Diboronic Acid 7b

Yield 81%. ^{1}H NMR ($CD_3OD + CDCl_3$) δ 8.40–8.36 (m, 4H), 8.25–8.22 (m, 4H), 7.82–7.18 (m, 20H), 5.69 (s, 4H), 4.89 (s, 4H), 4.08 (s, 4H), 3.75 (s, 4H), 2.54 (s, 6H), 2.25 (s, 6H). IR (cm^{-1}): 1637. MS-ESI: 478.4 ($M^+ + 2H$)/2. Elemental analysis calculated for $C_{60}H_{60}B_2N_4O_6{\cdot}2.4H_2O$: C, 72.21; H, 6.49; N, 5.61. Found: C, 71.96; H, 6.19; N, 5.39.

Diboronic Acid 7c

Yield 38%. ^{1}H NMR ($CD_3OD + CDCl_3$) δ 8.32–8.29 (m, 4H), 8.26–8.21 (m, 4H), 7.80–7.22 (m, 16H), 7.00 (s, 4H), 5.63 (s, 4H), 4.99 (s, 4H), 4.78 (s, 4H), 4.33 (s, 4H), 2.40 (s, 6H), 2.37 (s, 6H). IR (cm^{-1}): 1655. MS-ESI: 494.4 ($M^+ + 2H$)/2.

Diboronic Acid 7d

Yield 69%. ^{1}H NMR ($CD_3OD + CDCl_3$) δ 8.35–8.32 (m, 4H), 8.25–8.22 (m, 4H), 7.67–7.65 (m, 2H), 7.55–7.52 (m, 8H), 7.35–7.25 (m, 6H), 7.11 (s, 4H), 5.63 (s, 4H), 5.01 (s, 4H), 4.28 (s, 4H), 2.96 (t, J = 7.2 Hz, 4H), 2.64 (t, J = 7.2 Hz, 4H), 2.37 (s, 6H), 2.33 (s, 6H). IR (cm^{-1}): 1637. MS-ESI: 492.4 ($M^+ + 2H$)/2.

Diboronic Acid 7e

Yield 58%. ^{1}H NMR ($CD_3OD + CDCl_3$) δ 8.44–8.41 (m, 4H), 8.30–8.27 (m, 4H), 7.80–7.60 (m, 2H), 7.57–7.54 (m, 8H), 7.36–7.28 (m, 6H), 5.71 (s, 4H), 5.07 (s, 4H), 4.29 (s, 4H), 2.60 (s, 6H), 2.53 (t, J = 7.1 Hz, 4H), 2.39 (s, 6H), 2.15–2.10 (m, 2H). IR (cm^{-1}): 1632. MS-ESI: 875.7 ($M^+ - H_2O + H$). Elemental analysis calculated for $C_{55}H_{58}B_2N_4O_6{\cdot}H_2O$: C, 72.53; H 6.59; N, 6.15. Found: C, 72.19; H, 6.16; N, 5.76.

Diboronic Acid 7f

Yield 32%. ^{1}H NMR ($CD_3OD + CDCl_3$) δ 8.62–8.60 (m, 4H), 8.34–8.31 (m, 4H), 7.70–7.59 (m, 10H), 7.39–7.27 (m, 10H), 5.88 (s, 4H), 5.09 (s, 4H), 4.36 (s, 4H), 2.61 (s, 6H), 2.44 (s, 6H). IR (cm^{-1}): 1633. MS-ESI: 909.6 ($M^+ - H_2O + H$). Elemental analysis calculated for $C_{58}H_{56}B_2N_4O_6{\cdot}2H_2O$: C, 72.36; H, 6.23; N, 5.82. Found: C, 72.26; H, 5.75; N, 5.48.

Diboronic Acid 7g

Yield 71%. ^{1}H NMR ($CD_3OD + CDCl_3$) δ 8.31–8.28 (m, 4H), 8.18–8.15 (m, 4H), 7.56–7.50 (m, 8H), 7.40–7.30 (m, 8H), 5.65 (s, 2H), 5.57 (s, 4H), 4.90 (s, 4H), 4.26 (s, 4H), 3.18 (s, 4H), 2.33 (s, 6H), 2.16 (s, 6H). IR (cm^{-1}): 1642. MS-ESI: 887.6 ($M^+ - H_2O + H$). Elemental analysis calculated for $C_{56}H_{58}B_2N_4O_6$: C, 74.34; H, 6.46; N, 6.19. Found: C, 74.38; H, 6.73; N, 6.21.

Diboronic Acid 7h

Yield 50%. ^{1}H NMR ($CD_3OD + CDCl_3$) δ 8.49–8.46 (m, 4H), 8.24–8.22 (m, 4H), 7.80–7.60 (m, 2H), 7.57–7.54 (m, 8H), 7.36–7.28 (m, 6H), 5.70 (s, 4H), 4.96 (s, 4H), 4.33 (s, 4H), 2.78(s, 4H), 2.69 (s, 6H), 2.39 (s, 6H). IR (cm^{-1}): 1643, 1632. MS-ESI: 861.5 ($M^+ - H_2O + H$).

Diboronic Acid 7i

Yield 49%. ^{1}H NMR ($CD_3OD + CDCl_3$) δ 8.50–8.25 (m, 8H), 7.71–7.57 (m, 10H), 7.35–7.28 (m, 6H), 5.73 (s, 4H), 5.16 (s, 4H), 4.30 (s, 4H), 2.59 (s, 6H), 2.47 (s, 6H), 2.39 (t, J = 7.3 Hz, 4H), 1.80–1.60 (m, 4H), 1.50–1.35 (m, 4H). IR (cm^{-1}): 1632. MS-ESI: 917.5 ($M^+ - H_2O + H$).

Diboronic Acid 7j

Yield 30%. ^{1}H NMR ($CD_3OD + CDCl_3$) δ 8.45–8.43(m, 4H), 8.28–8.26 (m, 4H), 7.67–7.59 (m, 10H), 7.38–7.36 (m, 6H), 5.70 (s, 4H), 5.11 (s, 4H), 4.39 (s, 4H), 2.59 (s, 6H), 2.50–2.38 (m, 10H), 1.66–1.61 (m, 4H), 1.40–1.18 (m, 32H). IR (cm^{-1}): 1649, 1632. MS-ESI: 1113.8 ($M^+ - H_2O + H$).

Diboronic Acid 7k

Yield 50%. ^{1}H NMR ($CD_3OD + CDCl_3$) δ 8.50–8.34 (m, 8H), 7.71–7.61 (m, 12H), 7.45–7.34 (m, 8H), 5.86 (s, 4H), 5.06 (s, 4H), 4.24 (s, 4H), 2.57 (s, 6H), 2.42 (s, 6H). IR (cm^{-1}): 1631, 1620. MS-ESI: 909.5 ($M^+ - H_2O + H$).

Diboronic Acid 7l

Yield 40%. ^{1}H NMR ($CD_3OD + CDCl_3$) δ 8.46–8.30 (m, 8H), 8.29–7.56 (m, 10H), 7.28–7.26 (m, 8H), 7.10–6.90 (m, 2H), 5.89 (s, 2H), 5.76 (s, 2H), 5.16 (s, 2H), 5.12 (s, 2H), 4.90 (s, 2H), 4.38 (s, 2H), 4.35 (s, 2H), 2.68 (s, 3H), 2.63 (s, 3H), 2.46 (s, 3H), 2.42 (s, 3H). IR (cm^{-1}): 1632, 1608. MS-ESI: 939.5 ($M^+ - H_2O + H$).

Diboronic Acid 7m

Yield 42%. ^{1}H NMR (CD_3OD) δ 8.50–8.38 (m, 4H), 8.32–8.24 (m, 4H), 7.74–7.64 (m, 2H), 7.62–7.54 (m, 6H), 7.40–7.20 (m, 8H), 5.68 (s, 4H), 5.06 (s, 4H), 4.37 (s, 4H), 2.58 (s, 6H), 2.50–2.34 (m, 4H), 2.46 (s, 6H), 1.70–1.48 (m, 4H), 1.40–1.20 (m, 16H). ESI-MS: 1001.7 ($M^+ - H_2O + H$).

Diboronic Acid 7n

Yield 76%. ^{1}H NMR ($CD_3OD + CDCl_3$) δ 8.45–7.10 (m, 32H), 5.80 (s, 4H), 4.70 (s, 4H), 4.35 (s, 4H), 2.25 (s, 12H). ESI-MS: 985.6 ($M^+ - H_2O + H$).

Diboronic Acid 7o

Yield 89%. ^{1}H NMR ($CD_3OD + CDCl_3$) δ 8.60–8.50 (m, 4H), 8.40–8.24 (m, 4H), 7.90–7.20 (m, 24H), 5.90 (s, 4H), 4.94 (s, 4H), 4.20 (s, 4H), 2.62 (s, 6H), 2.40 (s, 6H). ESI-MS: 985.6 ($M^+ - H_2O + H$).

Diboronic Acid 7p
Yield 78%. ^{1}H NMR (CD_3OD + $CDCl_3$) δ 8.50–8.36 (m, 4H), 8.32–8.16 (m, 4H), 7.74–7.44 (m, 10H), 7.42–7.20 (m, 6H), 5.64 (s, 4H), 4.99 (s, 4H), 4.35 (s, 4H), 2.42–2.30 (m, 4H), 2.41 (s, 6H), 2.37 (s, 6H), 1.70–1.54 (m, 4H), 1.46–1.32 (m, 2H). IR (cm^{-1}): 1639. MS-ESI: 949.5 (M^+ + 2MeOH − $2H_2O$ + H).
Diboronic Acid 7q
Yield 70%. ^{1}H NMR (CD_3OD) δ 8.60–8.40 (m, 4H), 8.32–8.20 (m, 4H), 7.72–7.52 (m, 12H), 7.50–7.20 (m, 8H), 5.81 (s, 4H), 5.06 (s, 4H), 4.34 (s, 4H), 2.47 (s, 6H), 2.39 (s, 6H). IR (cm^{-1}): 1626. MS-ESI: 969.5 (M^+ + 3MeOH − $3H_2O$ + H). Elemental analysis calculated for $C_{58}H_{56}B_2N_4O_6{\cdot}2H_2O$: C, 72.28; H, 6.07; N, 5.82. Found: C, 72.27; H, 6.05; N, 5.87.
Diboronic Acid 7r
Yield 65%. ^{1}H NMR (CD_3OD) δ 8.60–8.42 (m, 4H), 8.40–8.30 (m, 4H), 7.80–7.52 (m, 10H), 7.50–7.20 (m, 10H), 7.15–7.00 (m, 4H), 5.81 (s, 4H), 5.04 (s, 4H), 4.35 (s, 4H), 2.54 (s, 6H), 2.40 (s, 6H). IR (cm^{-1}): 1616. MS-ESI: 1029.5 (M^+ + 2MeOH–$3H_2O$ + H).
Diboronic Acid 7s
Yield 58%. ^{1}H NMR (CD_3OD) δ 8.55–8.50 (m, 4H), 8.40–8.25 (m, 4H), 7.72–7.52 (m, 8H), 7.44–7.20 (m, 8H), 5.77 (s, 4H), 5.16 (s, 4H), 4.40 (s, 4H), 2.86–2.78 (m, 2H), 2.64 (s, 6H), 2.47 (s, 6H), 2.20–2.08 (m, 2H), 1.70–1.56 (m, 2H). IR (cm^{-1}): 1634. MS-ESI: 961.5 (M^+ + 2MeOH − $2H_2O$ + H).
Diboronic Acid 7t
Yield 70%. ^{1}H NMR (CD_3OD) δ 8.50–8.40 (m, 4H), 8.38–8.24 (m, 4H), 7.76–7.52 (m, 10H), 7.40–7.24 (m, 6H), 5.70 (s, 4H), 5.10 (s, 4H), 4.40 (s, 4H), 2.80–2.62 (m, 2H), 2.66 (s, 6H), 2.44 (s, 6H), 1.90–1.74 (m, 2H), 1.70–1.60 (m, 2H). IR (cm^{-1}): 1634. MS-ESI: 960.4 (M^+ + 2MeOH − $2H_2O$). Elemental analysis calculated for $C_{58}H_{62}B_2N_4O_6{\cdot}3H_2O$: C, 70.59; H, 6.95; N, 5.82. Found C, 70.56; H, 6.35; N, 5.81.
Diboronic Acid 7u
Yield 31%. ^{1}H NMR (CD_3OD + $CDCl_3$) δ 8.68–8.50 (m, 4H), 8.33–8.31 (m, 4H), 7.92–7.90 (m, 4H), 7.65–7.62 (m, 12H), 7.34–7.20 (m, 6H), 5.93 (s, 4H), 5.10 (s, 4H), 4.35 (s, 4H), 2.59 (s, 6H), 2.43 (s, 6H). IR (cm^{-1}): 1613. MS-ESI: 959.4 (M^+ − H_2O + H).
Diboronic Acid 7v
Yield 49%. ^{1}H NMR (CD_3OD + $CDCl_3$) δ 8.42–8.40 (m, 4H), 8.29–8.26 (m, 4H), 7.69 (m, 2H), 7.60–7.55 (m, 8H), 7.37–7.25 (m, 8H), 5.82 (s, 4H), 5.02 (s, 4H), 4.31 (s, 4H), 2.76 (s, 6H), 2.39 (s, 6H). IR (cm^{-1}): 1614. MS-ESI: 915.4 (M^+ − H_2O + H).
Diboronic Acid 7w
Yield 65%. ^{1}H NMR (CD_3OD + $CDCl_3$) δ 8.53–8.49 (m, 4H), 8.33–8.31 (m, 4H), 7.68–7.60 (m, 10H), 7.37–7.22 (m, 9H), 5.84 (s, 4H), 5.07 (s, 4H), 4.33 (s, 4H), 2.56 (s, 6H), 2.41 (s, 6H). IR (cm^{-1}): 1631. MS-ESI: 910.4 (M^+ − H_2O + H).
Diboronic Acid 7x
Yield 45%. ^{1}H NMR (CD_3OD + $CDCl_3$) δ 8.44–8.40 (m, 4H), 8.32–8.22 (m, 4H), 7.78–7.64 (m, 2H), 7.58–7.56 (m, 8H), 7.37–7.28 (m, 6H), 5.69 (s, 4H), 5.08 (s, 4H), 4.31 (s, 4H), 2.60 (s, 6H), 2.44–2.37 (m, 10H), 1.80–1.60 (m, 4H), 1.35–1.27 (m, 20H). IR (cm^{-1}): 1637. MS-ESI: 1029.6 (M^+ − H_2O + H).
Diboronic Acid 7y
Yield 91%. ^{1}H NMR (CD_3OD + $CDCl_3$) δ 8.40–7.40 (m, 24H), 5.63 (s, 4H), 4.70 (s, 4H), 4.10 (s, 4H), 2.56 (s, 6H), 2.47 (t, J = 7.0 Hz, 4H), 2.30 (s, 6H), 1.99–1.60 (m, 4H). ESI-MS: 889.6 (M^+ − H_2O + H). Elemental analysis calculated. for $C_{56}H_{60}B_2N_4O_6$: C, 74.18; H, 6.67; N, 6.18. Found C, 74.55; H, 7.00; N, 5.75.
Diboronic Acid 7z
Yield 98%. ^{1}H NMR (CD_3OD + $CDCl_3$) δ 8.66–8.58 (m, 4H), 8.24–8.08 (m, 4H), 8.00–7.20 (m, 22H), 6.10-5.74 (m, 4H), 4.80 (s, 4H), 4.19 (s, 4H), 2.36 (s, 6H), 2.29 (s, 6H). ESI-MS: 959.5 (M^+ − H_2O + H).

Biology

Cell Culture

HEPG2 and COS7 cells were maintained in RPMI with 10% FBS (GIBCO). HEP3B cells were maintained in RPMI with 10% FBS and 1× sodium pyruvate and 1× nonessential amino acids (GIBCO).

Flow Cytometry Analysis

Cell lines HEPG2, HEP3B, and COS7 were prepared and stained with monoclonal anti-carbohydrate antibodies at saturating concentrations as described (13, 14). Anti-SSEA-1 (anti-Lewis X) was used at a dilution of 1:1000, anti-Lewis Y (clone F3, Calbiochem, and clone A70-C/C8, NeoMarkers) at a dilution of 1:20, anti-sialyl Lewis X (CSLEX-1 and KM93) at 10 μg/ml, and anti-sialyl Lewis a (CSLEA-1) at 1:500. Cells were then stained with fluorescein isothiocyanate-conjugated goat anti-mouse IgM or anti-mouse IgG. FITC-conjugated murine IgG1/IgG2 and anti-CD18 antibodies (negative controls throughout) were used according to the manufacturer's instructions. Cells were analyzed on a Becton-Dickinson FACScan as previously described (13, 14).

Fluorescent Labeling Studies

Six-well plates were seeded with 1×10^6 cells per well and incubated at 37°C and 5% CO_2 for 48 hr. The media was removed and cells were washed twice with 1× PBS. The cells were fixed with 1.5 ml of 1:1 methanol/PBS and incubated 20 min at 4°C. After incubation, the methanol/PBS solution was removed and cells were washed twice with PBS.

Diboronic acid compounds were resuspended in 1:1 methanol/PBS and added to wells at 0.5–10 μM concentrations. One well was incubated only in methanol/PBS without compound as a negative control. The plates were then incubated in darkness at 4°C for 45 min. Plates were examined with phase contrast microscopy followed by fluorescent microscopy (blue cube wavelengths 370 nm excitation, 426 nm emission; 20X lens). Plates were photographed using a Nikon DXM1200 digital camera and images captured with the Nikon ACT-1 program (v 2.10). The phase contrast and fluorescent images were then overlaid, organized and labeled using Adobe Photoshop 6.0. The images were quantified with NIH ImageJ 1.28. The units (mean gray value) were subtracted from background, where there are no cells. The fluorescent signal was stable for at least 96 hr when cells were maintained in darkness.

Neuraminidase and Fucosidase Studies

HEPG2 cells (sLex-expressing) were treated with neuraminidases specific for α (2,3) sialic acid linkages (MDL number MFCD01092203, SIGMA #N7271) and α (2,3)/α (2,6) sialic acid residues (MDL number MFCD01092201, SIGMA #N5521) according to modifications of manufacturer's protocols. Incubations were performed in 20 mM Tris-HCL (pH 7.5) 25 mM NaCl (5× reaction buffer is 250 mM sodium phosphate [pH 6.0]) at 37°C for four hours. Control HEPG2 were treated with buffer alone at the same conditions. Incubation of cells with fucosidase recognizing α (1,3)- and (1,4) –linked fucose (MDL number MFCD00130491, SIGMA #F3023) were performed using the same buffers and conditions except the phosphate buffer is at pH 5.0. Incubation with both α (1,3/1,4)fucosidase (F3023) and α (2,3)neuraminidase (N7271) were performed with the same buffers and conditions except the pH was 5.5. The cells were then stained with **7q** and controls, examined under fluorescent microscopy, and photographed as above.

Acknowledgments

We gratefully acknowledge the financial support from the National Institutes of Health (NO1-CO-27184, CA88343, and DK55062) and North Carolina Biotechnology Center (2001ARG0016). The authors wish to thank Bihui Zeng for expert assistance with cell labeling experiments.

References

1. Fukuda, M. (1992). Cell Surface Carbohydrates and Cell Development. (Boca Raton: CRC).
2. Fukuda, M. (1994). Cell surface carbohydrates: Cell-type specific expression. In Molecular Glycobiology, M. Fukuda, and O. Hindsgaul, eds. (New York: Oxford University), pp. 1–52.
3. Fukuda, M. (1992). Cell surface carbohydrates in hematopoietic cell differentiation and malignancy. In Cell Surface Carbohydrates and Cell Development, M. Fukuda, ed. (Boca Raton: CRC), pp 127–160.
4. Dennis, J.W. (1992). Changes in glycosylation associated with malignant transformation and tumor progression. In Cell Surface Carbohydrates and Cell Development, M. Fukuda, ed. (Boca Raton: CRC), pp. 161–194.
5. Jorgensen, T., Berner, A., Kaalhus, O., Tveter, K.J., Danielsen, H.E., and Bryne, M. (1995). Up-regulation of the oligosaccharide

sialyl Lewis X: A new prognostic parameter in metastatic prostate cancer. Cancer Res. *55*, 1817–1819.
6. Idikio, H.A. (1997). Sialyl Lewis X, gleason grade and stage in nonmetastatic human prostate cancer. Glycoconj. J. *14*, 875–877.
7. El-Serag, H.B., and Mason, A.C. (1999). Rising incidence of hepatocellular carcinoma in the United States. N. Engl. J. Med. *340*, 745–750.
8. Shacter, E., and Weitzman, S.A. (2002). Chronic inflammation and cancer. Oncology *16*, 217–223.
9. Yago, K., Zenita, K., Ginya, H., Sawada, M., Ohmori, K., Minoru, O., Kannagi, R., and Lowe, J. (1993). Expression of alpha(1,3)-fucosyltransferases which synthesize sialyl Le(x) and sialyl Le(a), the carbohydrate ligands for E- and P-selectins in human malignant cell lines. Cancer Res. *53*, 5559–5565.
10. Goenner, S., Cosson, C., Boutron, A., Legrand, A., and Moatti, N. (1997). Interleukin-1 and interleukin-6 stimulate 2-methyl-aminoisobutyric acid uptake in HEPG2 cells. Int. J. Biochem. Cell Biol.. *29*, 667–674.
11. Mackiewicz, A., Speroff, T., Ganapathi, M.K., and Kushner, I. (1991). Effects of cytokine combinations on acute phase protein production in two hepatoma cell lines. J. Immunol. *146*, 3032–3037.
12. Minta, J.O., Fung, M., and Paramasawara, B. (1998). Transcriptional and post-transcriptional regulation of complement factor I (CFI) gene expression in HEPG2 cells by interleukin-6. Biochim. Biophys. Acta *1442*, 286–295.
13. Nakaya, R., Kohgo, Y., Mogi, Y., Kakajima, M., Kato, J., and Niitsu, Y. (1994). Regulation of asialoglycoprotein receptor synthesis by inflammation-related cytokines in HEPG2 cells. J. Gastroenterol. *29*, 24–30.
14. Brinkman-Van der Linden, E.C.M., Mollicone, R., Oriol, R., Larson, G., Van der Eijnden, D.H., and Van Dijk, W. (1996). A missense mutation in the FUT6 gene results in total absense of alpha3-fucosylation of human alpha1-acid glycoprotein. J. Biol. Chem. *271*, 14492–14495.
15. Mita, Y., Aoyagi, Y., Suda, T., and Asakura, H. (2000). Plasma fucosyltransferase activity in patients with hepatocellular carcinoma, with special reference to correlation with fucosylated species of alpha-fetoprotein. J. Hepatol. *32*, 946–954.
16. Fujiwara, Y., Shimada, M., Takenaka, K., Kajiyama, K., Shirabe, K., and Sugimachi, K. (2002). The sialyl Lewis X expression in hepatocarcinogenesis: potential predictor for the emergence of hepatocellular carcinoma. Hepatogastroenterology *49*, 213–217.
17. Nakakura, E.K., and Choti, M.A. (2000). Management of hepatocellular carcinoma. Oncology *14*, 1085–1098.
18. Yang, W., Gao, S., Gao, X., Karnati, V., Ni, W., Wang, B., Hooks, W.B., Carson, J., and Weston, B. (2002). Diboronic acids as fluorescent probes for cells expressing sialyl Lewis X. Bioorg. Med. Chem. Lett. *12*, 2175–2177.
19. Weston, B.W., Hiller, K.M., Mayben, J.P., Manousos, G.A., Bendt, K.M., Liu, R., and Cusack, J.C., Jr. (1999). Expression of human a(1,3)fucosyltransferase antisense sequences inhibits selectin-mediated adhesion and liver metastasis of colon carcinoma cells. Cancer Res. *59*, 2127–2135.
20. Lorand, J.P., and Edwards, J.O. (1959). Polyol complexes and structure of the benzeneboronate ion. J. Org. Chem. *24*, 769–774.
21. Wang, W., Gao, X., and Wang, B. (2002). Boronic acid-based sensors for carbohydrates. Curr. Org. Chem. *6*, 1285–1317.
22. Yang, W., Gao, X., and Wang, B. (2003). Boronic acid compounds as potential pharmaceutical agents. Med. Res. Rev. *23*, 346–368.
23. James, T.D., Sandanayake, K.R.A.S., Iguchi, R., and Shinkai, S. (1995). Novel saccharide-photoinduced electron transfer sensors based on the interaction of boronic acid and amine. J. Am. Chem. Soc. *117*, 8982–8987.
24. James, T.D., Sandanayake, K.R.A.S., and Shinkai, S. (1995). Chiral discrimination of monosacchrides using a fluorescent molecular sensor. Nature *374*, 345–347.
25. Eggert, H., Frederiksen, J., Morin, C., and Norrild, J.C. (1999). A new glucose-selective fluorescent bisboronic acid. First report of strong a-furanose complecation in aqueous solution at physiological pH. J. Org. Chem. *64*, 3846–3852.
26. Adhikiri, D.P., and Heagy, M.D. (1999). Fluorescent chemosensor for carbohydrates which shows large change in chelation-enhanced quenching. Tetrahedron Lett. *40*, 7893–7896.
27. Wiskur, S.L., and Anslyn, E.V. (2001). Using a synthetic receptor to create an optical-sensing ensemble for a class of analytes: A colorimetric assay for the aging of scotch. J. Am. Chem. Soc. *123*, 10109–10110.
28. Tong, A.-J., Yamauchi, A., Hayashita, T., Zhang, Z.-Y., Smith, B.D., and Teramae, N. (2001). Boronic acid fluorophore/beta-cyclodextrin complex sensors for selective sugar recognition in water. Anal. Chem. *73*, 1530–1536.
29. Yang, W., He, H., and Drueckhammer, D.G. (2001). Computer-guided design in molecular recognition: Design and synthesis of a glucopyranose receptor. Angew. Chem. Int. Ed. Engl. *40*, 1714–1718.
30. DiCesare, N., and Lakowicz, J.R. (2001). New color chemosensors for monosaccharides based on azo dyes. Org. Lett. *3*, 3891–3893.
31. Ward, C.J., Patel, P., and James, T.D. (2002). Molecular color sensors for monosaccharides. Org. Lett. *4*, 477–479.
32. Springsteen, G., and Wang, B. (2002). A detailed examination of boronic acid-diol complexation. Tetrahedron *58*, 5291–5300.
33. Wang, W., Gao, S., and Wang, B. (1999). Building fluorescent sensors by template polymerization: the preparation of a fluorescent sensor for D-fructose. Org. Lett. *1*, 1209–1212.
34. Gao, S., Wang, W., and Wang, B. (2001). Building fluorescent sensors for carbohydrates using template-directed polymerizations. Bioorg. Chem. *29*, 308–320.
35. Sugasaki, A., Sugiyasu, K., Ikeda, M., Takeuchi, M., and Shinkai, S. (2001). First successful molecular design of an artificial Lewis oligosaccharide binding system utilizing positive homotropic allosterism. J. Am. Chem. Soc. *123*, 10239–10244.
36. Wulff, G. (1982). Selective binding to polymers via covalent bonds–The construction of chiral cavities as specific receptor-sites. Pure Appl. Chem. *54*, 2093–2102.
37. Karnati, V.R., Gao, X., Gao, S., Yang, W., Ni, W., Sankar, S., and Wang, B. (2002). A glucose-selective fluorescence sensor based on boronic acid-diol recognition. Bioorg. Med. Chem. Lett. *12*, 3373–3377.
38. Lin, Y.-I., Lang, S.A., Seifert, C.M., Child, R.G., Morton, G.O., and Fabio, P.F. (1979). Aldehyde syntheses. Study of the preparation of 9,10-anthracenedicarboaldehyde. J. Org. Chem. *44*, 4701–4703.
39. Okada, Y., Jin-no, K., Ikeda, H., Sakai, N., Sotozono, M., Yonei, T., Nakanishi, S., Moriwaki, S., and Tsuji, T. (1994). Changes in the expression of sialyl-Lewis^x, a hepatic necroinflammation-associated carbohydrate neoantigen, in human hepatocellular carcinomas. Cancer *73*, 1811–1816.
40. Jezequel-Cuer, M., Dalix, A.M., Flejou, J.F., and Durand, G. (1992). Variations in human liver fucosyltransferase activities in hepatobiliary diseases. Liver *12*, 140–146.
41. Sasaki, M., Kono, N., and Nakanuma, Y. (1994). Neoexpression of Lewis Y antigen is a sensitive phenotypic change of the damaged intrahepatic bile ducts. Hepatology *19*, 138–144.
42. Hiller, K.M., Mayben, J.P., Bendt, K.M., Manousos, G.A., Singer, K., Cameron, H.S., and Weston, B.W. (2000). Transfection of alpha(1,3)fucosyltransferase antisense sequences impairs the proliferative and tumorigenic ability of human colon carcinoma cells. Mol. Carcinog. *27*, 280–288.
43. Weston, B.W., Nair, R.P., Larsen, R.D., and Lowe, J.B. (1992). Isolation of a novel human alpha(1,3)fucosyltransferase gene and molecular comparison to the human Lewis blood group alpha(1,3/1,4)fucosyltransferase. J. Biol. Chem. *267*, 4152–4160.
44. Weston, B.W., Smith, P.L., Kelly, R.J., and Lowe, J.B. (1992). Molecular cloning of a fourth member of a human alpha(1,3)fucosyltransferase gene family. J. Biol. Chem. *267*, 24575–24584.